ACS APPLIED MATERIALS & INTERFACES

Research Article

www.acsami.org

Dual-Biomimetic Superhydrophobic Electrospun Polystyrene Nanofibrous Membranes for Membrane Distillation

Xiong Li,[†] Ce Wang,[†] Yin Yang,[†] Xuefen Wang,*[,†] Meifang Zhu,*[,†] and Benjamin S. Hsiao[‡]

[†]State Key Lab for Modification of Chemical Fibers and Polymer Material, Donghua University, Shanghai, 201620, P.R. China

[‡]Department of Chemistry, Stony Brook University, Stony Brook, New York 11794, United States

Supporting Information

ABSTRACT: A new type of dual-biomimetic hierarchically rough polystyrene (PS) superhydrophobic micro/nano-fibrous membrane was fabricated via a one-step electrospinning technique at various polymer concentrations from 15 to 30 wt %. The obtained micro/nano-fibers exhibited a nanopapillose, nanoporous, and microgrooved surface morphology that originated from mimicking the micro/nanoscale hierarchical structures of lotus leaf and silver ragwort leaf, respectively. Superhydrophobicity and high porosity of such resultant electrospun nanofibrous membranes make them attractive candidates for membrane distillation (MD) application with low energy water recovery. In this study, two kinds of optimized PS nanofibrous membranes with different thicknesses were applied for desalination via direct contact MD. The membranes maintained a high and stable permeate water vapor flux (104.8 ± 4.9 kg/m^2·h, 20 g/L NaCl salt feed for a thinner PS nanofibrous membrane with thickness of 60 μm; 51 ± 4.5 kg/m^2·h, 35 g/L NaCl salt feed for the thicker sample with thickness of 120 μm; ΔT = 50 °C) for a test period of 10 h without remarkable membrane pores wetting detected. These results were better than those of typical commercial polyvinylidene fluoride (PVDF) MD membranes or related PVDF nanofibrous membranes reported in literature, suggesting excellent competency of PS nanofibrous membranes for MD applications.

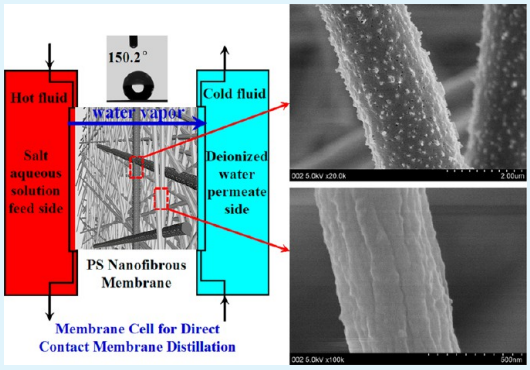

KEYWORDS: *superhydrophobic, polystyrene, nanofibrous membrane, membrane distillation*

INTRODUCTION

Membrane distillation (MD) is a thermally-driven non-isothermal membrane separation process, in which only vapor molecules can transfer through a high hydrophobic microporous membrane. The driving force in the MD process is the vapor pressure difference induced by the temperature difference between the feed and permeate side.[1−3] In general, four different MD configurations including direct contact MD, sweeping gas MD, vacuum MD, and air gap MD have been applied to desalination, environmental/waste treatment, food industry, etc.[4−8] Significantly, direct contact MD is the most popular and simplest operation mode, and over 60% of MD studies are carried out using direct contact MD systems.[2]

Basically, a good MD performance is evaluated by the selectivity (rejection or permeate conductivity which depends on the superhydrophobicity) and permeability (permeate vapor flux) of the MD membrane. Thus, the MD membrane should possess sufficient hydrophobicity, a small mean flow pore size (MFP) and a narrow pore size distribution to obtain a high liquid entry pressure of water (LEPw, was commonly characterized as the ability of the membrane to hinder any liquid water penetrate into pores) and to prevent membrane pores wetting.[8] Furthermore, microporosity and excellent breathability of the membrane (provides abundant interconnected pores to the transmission of permeate water vapors) are also very important for achieving higher permeate vapor flux during MD operation, the compromise can be made by constructing a high porosity of web configuration with an appropriate MFP and pore size distribution.[2,9,10] Interestingly, the versatile and effective electrospinning technique provides an ideal strategy for the construction of superhydrophobic nanofibrous membranes with highly porous web structure and controllable pore size. Hence, the resultant superhydrophobic electrospun nanofibrous membranes exhibiting several attractive characters could fulfill the MD membrane requirements, such as high porosity, interconnected porous structure, enormous surface-to-mass/volume ratio, uniform fiber morphology with controllable pore size, etc.[11−14] Examples of superhydrophobic electrospun nanofibrous membranes applied for water desalination via direct contact MD include the superhydrophobic aromatic fluorinated polyazole, PVDF, and PVDF blended with clay nanocomposites nanofibrous mats with stable water-repellency to assure the MD performance with excellent permeability and selectivity.[12,15,16]

Manufacturing bio-inspired superhydrophobic electrospun fibrous surfaces have gained substantial attention, which

Received: October 30, 2013
Accepted: January 27, 2014
Published: January 27, 2014

originated from mimicking the micro/nanoscale hierarchical structures of biological organisms from nature. For example, inspired by the self-cleaning lotus leaf, a biomimically designed superhydrophobic poly(ε-caprolactone) (PCL) surface was obtained using a modified electrostatic process, which exhibited a micrometer-sized pyramid structure consisting of accumulated droplets and nanofibers.[17] It is noteworthy that PS with a low surface energy has been widely used for electrospun superhydrophobic fibrous mat surface. Lu et al.[18] reported a PS-ionic liquid composite nanofibrous membrane with both superhydrophobicity and conductivity, and Zhu et al.[19] have also shown a stable superhydrophobic and conductive polyaniline/polystyrene composite film for many corrosive environments. Besides the lotus leaf, the silver ragwort leaf also exhibits the water-repellency and self-cleaning property. Ding's group has successfully constructed a silver-ragwort-leaf-like micro/nanoscaled roughness on PS fiber surfaces by tuning the solvent composition ratios of tetrahydrofuran (THF) to *N*,*N*′-dimethylformamide (DMF) in PS solutions.[20,21] Furthermore, Ding et al.[22] have demonstrated the fabrication of dual-biomimetic superhydrophobic electrospun fiber surfaces in the presence of silica nanoparticles, which exhibited a fascinating structure with the combination of nano-protrusions and numerous grooves, inspired by the lotus leaf and silver ragwort leaf. Although these techniques provide PS fabrics with great superhydrophobic surfaces, the MD applicability of such electrospun membranes without adequate structural attributes is limited.

Combined with the special wettability of the lotus leaf and silver ragwort leaf, the cooperation of their unique micro/nanoscale hierarchical surface structures and low surface energy materials is believed to be the reason for the superhydrophobicity. Herein, we describe a new type of dual-biomimetic PS superhydrophobic nanofibrous membrane with micro/nanoscaled roughness via a one-step electrospinning technique, which originated from imitating the micro/nanoscale hierarchical structures of lotus leaf and silver ragwort leaf. Importantly, the obtained superhydrophobic PS nanofibrous membranes with excellent structural properties could be applied for desalination via direct contact MD, and exhibited a remarkable deionized water productivity triggered by avoiding the major obstacles for MD including membrane pores wetting and low permeate vapor flux.

EXPERIMENTAL SECTION

Electrospinning Details. Polystyrene (PS, M_W = 192 000 g/mol, from Sigma Aldrich) was dissolved in *N*,*N*′-dimethylformamide (DMF, was kindly supplied by Shanghai Chemical Reagent Plant) by mild stirring in an oil bath (~40 °C) for 24 h to obtain 15, 20, 25, and 30 wt % homogeneous transparent solution. About 5 mL of the PS/DMF solution was placed in a 5-mL syringe equipped with a blunt metal needle of 0.37 mm inner diameter. The syringe was placed in a syringe pump that maintained a solution feeding rate of 0.3 mL/h. A grounded drum covered with a piece of PET (polyethylene terephthalate) spunbonded nonwoven was used as collector, which rotated at 500 rpm. The distance between the needle tip and collector was 15 cm, and the voltage was set at 30 kV. Rabolt et al.[23,24] have reported that an increase in the number of pores on the PS fibers surface can be obtained by increasing the amount of humidity. Herein, the relevant temperature and humidity was controlled at 30 ± 2 °C and 30 ± 5%, respectively, for controlling the fine structure of the electrospun fiber properly and repeating easily. The obtained electrospun samples from the PS concentration of *x* wt % were denoted as PS-*x*. Here, it should be emphasized that a relative lower solution feeding rate and a relative higher applied voltage was employed in this work for generating stronger electrostatic force for enhancing the instability of the electrospinning jet resulting in the electrospun PS fibers with roughened microfibers and nanofibers together by contrast with the previous literatures reported uniform electrospun PS fibers from PS/DMF solutions.[25−28] For example, Jiang et al.[28] got uniform and smooth nanofibers from 25 wt % PS/DMF solution with feeding rate of 2 mL/h at a distance between the tip and collector of 14 cm and an applied voltage of 14 kV (no environmental control, and PS M_w = 220 000).

Characterization of Surface Morphology and Surface Property. The surface morphology of the electrospun samples were investigated by scanning electron microscopy (SEM) (JSM-5600LV, Japan) and field emission scanning electron microscopy (FESEM) (SU8000, Hitachi, Japan). The wettability of the surface was performed by a dynamic contact angle testing instrument (OCA40, Dataphysics, Germany). Average water contact angles were obtained by measuring the same sample at five different positions.

Characterizations of Electrospun PS Nanofibrous Membranes. PS fiber diameters together with its distribution were measured using an image analyzer, namely, ImageJ 2X software, 5 SEM images have been considered and the diameters of a total number of 200 fibers have been measured. Statistical analysis have been applied to determine the fiber diameter distribution and to estimate the arithmetic weighted mean of the fiber diameter together with its distribution.

The porosity of the membrane is defined as the volume of the pores divided by the total volume of the membrane,[29] which can be measured by gravimetric method. Isopropyl alcohol (IPA) was used as the wetting liquid which penetrated into the pores of the PS nanofibrous membrane, the membrane weight was measured before and after saturated by IPA. The membrane porosity, ε, can be calculated by the equation

$$\varepsilon = \frac{(w_w - w_d)/\rho_i}{(w_w - w_d)/\rho_i + w_d/\rho_p}$$

where w_d is the weight of the dry membrane, w_w is the weight of the wet membrane, ρ_i is the isopropyl alcohol density, and ρ_p is the polymer density.

A home-made experimental apparatus schematized in Figure 1[29] was used for liquid entry pressure of water (LEPw) measurements.

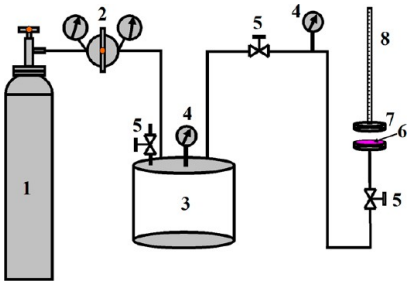

Figure 1. Apparatus for the determination of the LEPw: (1) gas cylinder with nitrogen, (2) reducing valve, (3) reservoir, (4) manometer, (5) pressure regulator, (6) membrane, (7) measuring cell, and (8) measuring pipette.

The dry PS nanofibrous sample with an effective area of 10 cm^2 was placed into the measuring cell and the reservoir was filled with deionized water. By means of a gas cylinder which was filled with nitrogen, a slight pressure was raised stepwise with 0.005 bar and each pressure was maintained for 10 min in the process of the degasification of the permeate side and the LEPw test. The minimum applied pressure which resulted in a continuous flux was regarded as the LEPw value.[29] The measurements were carried out thrice using three different membrane samples made under the same condition. The results were averaged to obtain the final LEPw value.

The mean flow pore size (MFP), pore size distribution, bubble point or maximum pore size of electrospun PS membranes were characterized by using a capillary flow porometer (Porolux 500) based on the wet/dry flow method, where the membrane samples were initially wetted with perfluoroether (Porefil, wetting liquid, with a defined surface tension of 16 dyn/cm) and subsequently placed in a sealed chamber through which gas (nitrogen) flows. The change in flow rate was measured as a function of pressure for both dry and wet processes. And the results were obtained by the following equation:[30]

$$P = \frac{4\gamma \cos\theta}{D}$$

where P is the differential pressure, γ is the surface tension of the wetting liquid, θ is the contact angle of the wetting liquid (in this case zero), and D is the pore diameter.

Gas flow rate measured through dry membrane samples yielded gas permeability.[30] According to Darcy's law, flow of fluids through porous media was proportional to the pressure gradient causing flow.[31]

Direct Contact Membrane Distillation. Two kinds of optimized PS nanofibrous membranes with different thicknesses and 0.2 commercial PVDF membrane (mean pore size 0.2 μm) were applied for direct contact MD test with an effective membrane area of 30 cm^2. The schematic diagram of the direct contact MD experimental setup is shown in Figure 2. In this study, the direct contact MD test was

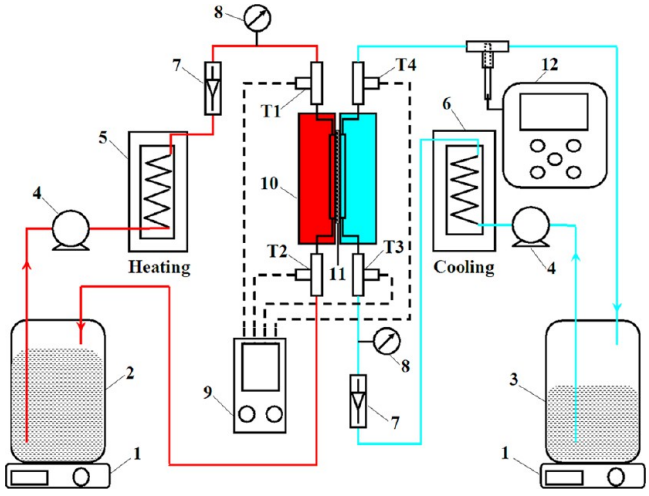

Figure 2. Schematic diagram of the direct contact MD setup: (1) digital balance, (2) feed solution, (3) permeate tank, (4) diaphragm laboratory pump, (5) heating system, (6) chiller, (7) flowmeter, (8) manometer, (9) thermometer, (T1−T4) temperature probe, (10) membrane cell, (11) membrane, and (12) conductivity meters.

conducted with NaCl aqueous solutions of different concentrations (0, 10, 20, and 35 g/L) as feed, and the permeate tank was deionized water (a conductivity of around 2.3 μs/cm). The feed temperature was varied from 30 to 75 °C (considering the glass transition temperature of PS is 80−100 °C) by one heating system and circulated by a diaphragm laboratory pump (0.2−1.3 L/min), while the permeate side was maintained at 20 °C by one chiller to condense the permeate vapors and circulated by another diaphragm laboratory pump. The flow rate at feed and permeate side was maintained at 0.6 L/min which was chosen based on the LEPw of the selected membranes. In consideration of the permeate vapor flux of commercial PVDF membrane was still very low from a relative higher flow rate,[32,33] and we also want to achieve a low energy water recovery MD process, thus we choose the same flow rate of 0.6 L/min for commercial PVDF membrane test. During the test, the conductivity of the feed and permeate solution were monitored by conductivity meters (SevenEasy, Mettler Toledo) and the permeate vapor flux was obtained by the weight increase of the permeate tank which was located on one digital balance (MS6001S, Mettler Toledo).

RESULTS AND DISCUSSION

Surface Morphology and Surface Property. The morphologies of the electrospun products are mainly influenced by the solution concentration at given electrospinning parameters. In the electrospinning process, the electrostatic force overcomes the surface tension of the polymer solution, resulting in the ejection of a thin jet from the pendent drop of polymer solution at the tip. The competition between the electrostatic force and the surface tension of the polymer solution decides the morphology of the product.[28] For dilute solution, the low viscosity is insufficient to sustain the elongation of the liquid jet, the thin jet of solution leaving the nozzle will shrinks to droplets and form microparticles. With the increase of solution concentration, bead-on-string structure will be observed. When the solution concentration increases to a certain degree, sufficient chain entanglement will serve to stabilize the electrospinning jet to favor the fiber formation. Figure 3 shows the representative SEM images of electrospun membranes prepared from different PS concentration. As can be seen from Figure 3A, for the dilute PS solution of 15 wt %, the morphology of electrospun PS-15 exhibited a microellipsoid/nanofiber composite structure. It could be observed that every microellipsoid is interlinked with nanofibers and contains lots of nanoscale protrusions, the nanofibers are randomly interwoven on the surfaces of the micro-ellipsoids, while the sizes of the microellipsoids are 3−10 μm and the diameters of nanofibers are in the range of 100−300 nm, respectively. Thus, this kind of hierarchical structures containing micro/nano-scaled roughness endowed the PS-15 with a water contact angle of 154.5 ± 1.6° (Figure 3F). With the increasing of PS concentration from 20 to 30 wt %, the surface morphology showed an elliptical bead-on-string structure to the uniform and smooth fiber (Figure 3B−D), whereas the corresponding water contact angle gradually decreased to 152.9 ± 1.4°, 150.2 ± 1.2°, and 126.6 ± 1.4°, respectively. In the case of electrospun PS-30 samples, the remarkable decline of water contact angle could be ascribed to the lack of any rough structure formation on the microfiber surface, and adhesions were clearly visible among the adjacent microfibers. The insufficient hydrophobicity and large fiber diameter of PS-30 surface limited their applicability as a competent MD membrane, as well as the PS-15 and PS-20 with inadequate structural integrity due to the existence of the fragile elliptical-beads with large sizes, in spite of their desired large water contact angles. It is noteworthy that PS-25 exhibited an optimized nanofiber morphology with relatively uniform fiber diameter (with the existence of a few microfibers) and still possessed good hydrophobic property.

To get a further observation of the relationship between surface wettability and the fine micro/nano-structure of electrospun PS-25 membranes, the high resolution representative FE-SEM images of electrospun PS-25 membranes were shown in Figure 4. As can be seen from Figure 4, a special dual-biomimetic hierarchically rough micro/nanostructural fibers were observed, inspired by the micro/nanoscale hierarchical structures of lotus leaf and silver ragwort leaf. The existence of microfibers caused by the axial-symmetric instability in the process of spin charged jet bending and stretching,[34] exhibited a nanopapillose (50−80 nm) and nanoporous (about 20 nm) surface morphology (indicated by dotted circle, Figure 4B and D), resulting from the retarded evaporation of the residual DMF trapped inside the microfibers.[35,36] The typically

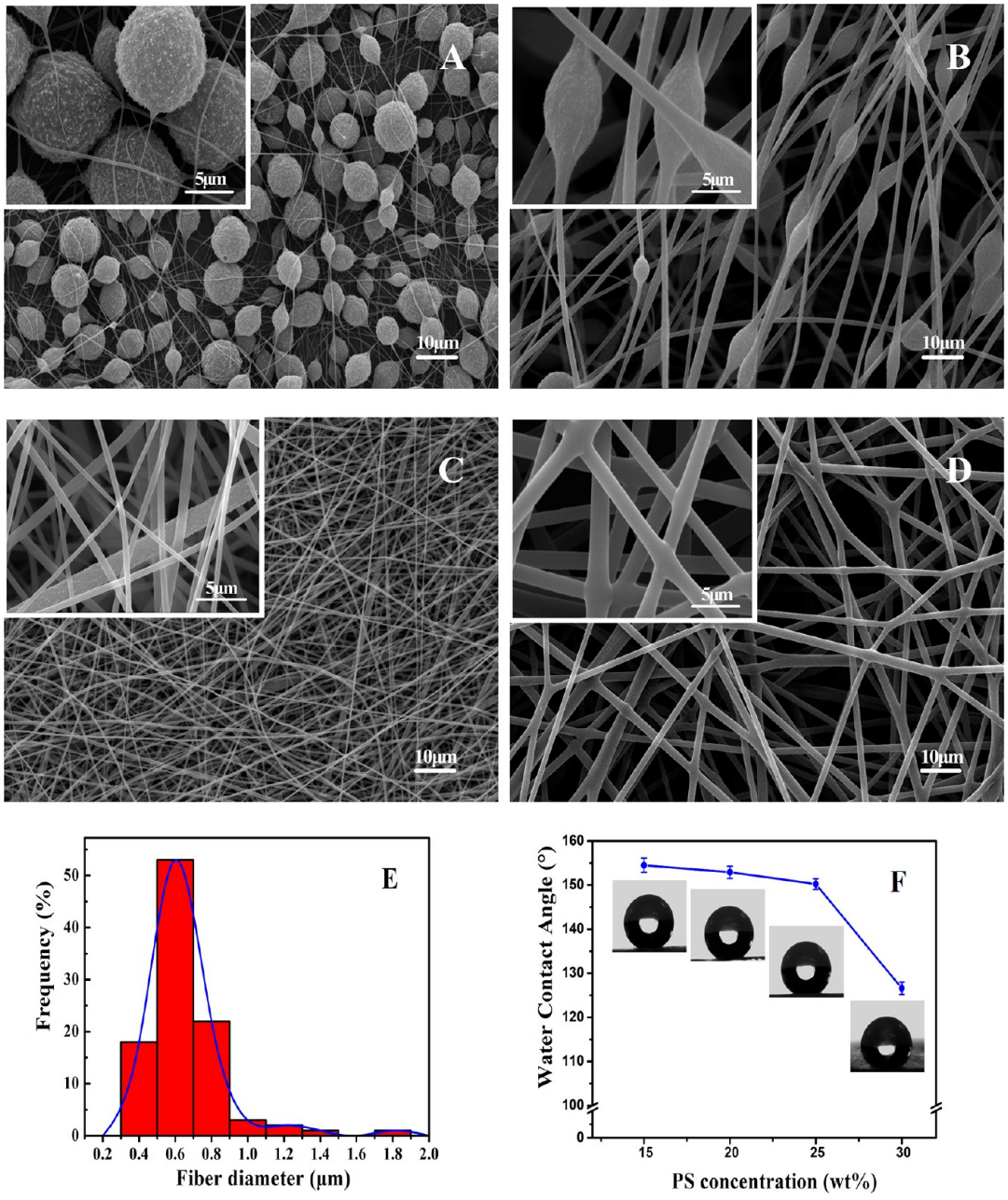

Figure 3. SEM images of (A) PS-15, (B) PS-20, (C) PS-25, and (D) PS-30. (E) Fiber diameter together with its distribution of PS-25. (F) Water contact angles for PS-15−30 nanofibrous membranes.

hierarchical structures of nanofibers with microgrooves along the fiber axis was successfully introduced by constructing micro-wrinkles on the nanofiber surface, and this unique surface topographies could be explained by the buckling instabilities associated with the solvent evaporation from the surface of the fluid jet and trapped inside the jet which resulted in a contraction mismatch.[37] A combination of both nanofibers and a very few microfibers with various hierarchical roughness endowed the electrospun PS-25 membrane with a water contact angle of 150.2 ± 1.2°.

Structural Attributes of Electrospun PS-25 Membranes. The optimized electrospun PS-25 nanofibrous membranes were cold-pressed at room temperature under 2 MPa pressure for 30 s to improve their dimensional integrity, then two samples with the thickness of 60 and 120 μm were selected to characterize their structural properties for the direct contact MD evaluation. An appropriate MFP and a narrow pore size distribution are suggested for the performance of MD membrane to prevent membrane pores wetting.[2] With respect to the Knudsen and viscous diffusion in the MD processes, a pore size range of 0.2−0.5 μm was preferred.[9] And for commercial phase inversion membranes currently used, the MFP ranged from 0.2 to 1 μm.[1] However, whether the fluorinated polytriazole electrospun nanofibrous membranes with a broad pore size distribution in the range of 2.5 to 3.3 μm and a MFP of 2.7 μm, or the PVDF-HFP nanofibrous membranes with a narrow pore size distribution ranging from 0.21 to 0.77 μm and a MFP of 0.26 μm, both of them could be used as MD membrane.[15,38] As shown in Figure 5A, electrospun PS-25 membrane with the thickness of 60 μm exhibited a narrow distribution of the pore diameter in the range of 0.33 to 1.35 μm with a MFP of 0.76 μm, nevertheless

dx.doi.org/10.1021/am4048128 | ACS Appl. Mater. Interfaces 2014, 6, 2423−2430

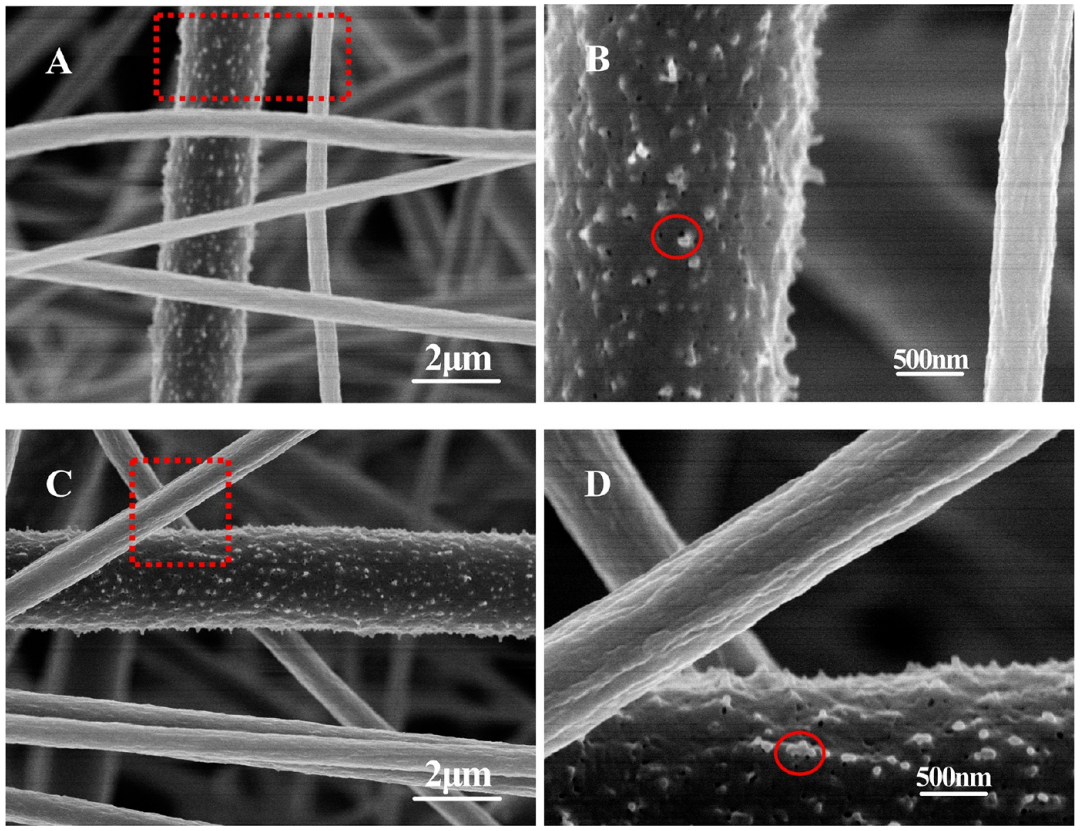

Figure 4. FE-SEM images of dual-biomimetic PS-25 nanofibrous membranes (A and C), corresponding to the magnified images (B and D) of the dotted lines. The dotted circles showed the nanopapillose and nanoporous structures.

the sample having a thickness of 120 μm contained a relatively broader pore size distribution ranging from 0.52 to 2.08 μm with a MFP of 1.15 μm. This could be due to the difference of the membrane compactness from the cold-pressing under the same pressure, that is, the thick PS-25 membrane was relatively looser than the thin one.

It is generally agreed upon that higher membrane porosity results in higher permeate vapor flux. And in general, the MD membrane porosity ranges from 30 to 85%.[39] As can be seen in Table 1, two kinds of optimized PS-25 nanofibrous membranes have reasonably high porosity required for MD application, which was 69% and 77.5%, respectively.

The flow rate at feed and permeate side was determined based on the LEPw value of the hydrophobic membranes. Compared with the PVDF commercial membrane with a high LEPw value (~2.91 bar),[38] the electrospun nanofibrous membranes generally exhibited a relatively lower LEPw value. For example, the electrospun PVDF, fluorinated polytriazole, PVDF-HFP, and PVDF/clay nanofibrous membranes presented the LEPw values of 0.35, 0.76, 1.32, and 2 bar, respectively.[15,16,38,40] The diversity of these LEPw values could be attributed to the different membrane pore size, membrane hydrophobicity, and porosity. In this study, the LEPw values of the electrospun PS-25 nanofibrous membranes with the thickness of 60 and 120 μm were 0.6 and 0.8 bar, respectively.

The gas permeability of the resultant membranes was another crucial factor for evaluating the permeate vapor flux through the membrane. During the direct contact MD test process, the permeate water vapors would be condensed into the cold fluid on the fluid-membrane interface by a circulated chiller system. As stated previously, the gas permeability can be calculated from the gas flow rate through the dry membrane samples by using a capillary flow porometer. For the two selected PS-25 nanofibrous membranes, the nitrogen permeability varies linearly with the nitrogen pressure, as shown in Figure 5B. The membrane with a thickness of 60 μm presented a little lower nitrogen permeability of 189.0 cm^3/s at 0.2 bar because of its narrow pore size distribution, as compared to the membrane with the thickness of 120 μm (249.3 cm^3/s at 0.2 bar). Notably, these gas permeability data were extremely higher than that of conventional commercial PVDF MD membranes (88.6 cm^3/s at 2.8 bar).[38]

Performance in Direct Contact MD Test. The optimized flat-sheet PS-25 samples were continuous tested for 10 h in a direct contact MD setup to examine their potential for MD application. According to the inversely proportional relationship between the membrane thickness and the permeate flux,[1,2,12,41] two samples with different thicknesses were chosen to investigate their suitability for different feed concentration. Comparison of the permeate vapor flux for the two PS-25 membranes with different thickness as a function of temperature difference (10−55 °C) at different NaCl salt concentrations (0, 10, 20, 35 g/L) was represented in Figure 6. A larger temperature difference and a lower NaCl salt concentration yielded a higher permeate vapor flux. A considerable increase of the permeate vapor flux with the temperature difference was attributed to the enhancement of the vapor pressure at the feed/PS-25 membrane interface and the temperature polarization effect.[3,10] Additionally, the permeate vapor flux decreased with the increase of NaCl salt concentration was ascribed to the reduction of the water vapor pressure at the feed/membrane interface and the concentration

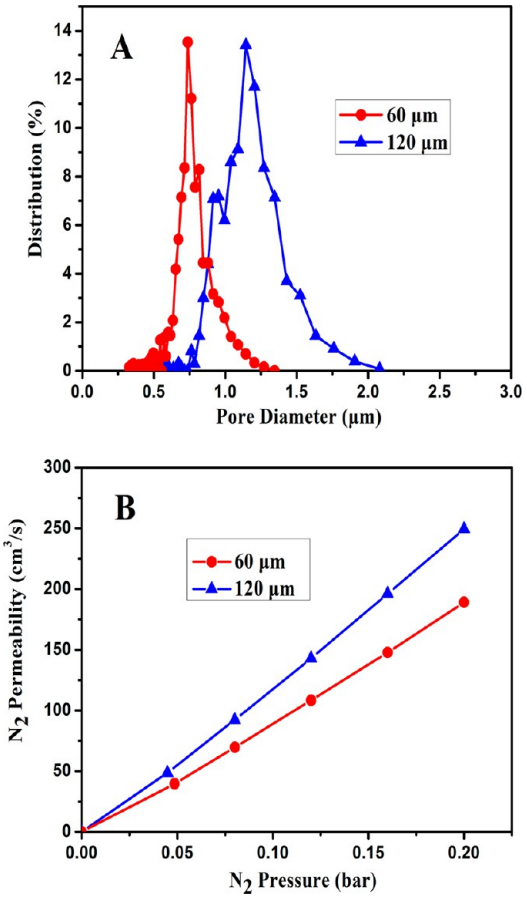

Figure 5. Pore size distribution (A) and gas permeability results (B) of PS-25 nanofibrous membranes with the thickness of 60 and 120 μm.

Table 1. Structural Attributes of PS-25 Nanofibrous Membranes

sample thickness (μm)	LEPw (bar)	porosity (%)	pore size range (μm)	MFP size (μm)	90% pore size (μm)
60	0.6	69	0.33−1.35	0.76	0.62
120	0.8	77.5	0.52−2.08	1.15	0.90

polarization effect.[3] The obtained trends in this study were well in accordance with those reported by Nunes[15] and Khayet[12] for the polyazole and PVDF nanofibrous membranes. It also can be seen from Figure 6 that, for PS-25 samples with the thickness of 60 μm at temperature difference of 55 °C, the highest vapor flux obtained was 161.2 ± 6.6, 152 ± 6.5 and 113 ± 6.9 kg/m^2·h, corresponding to the feed solution with different NaCl salt concentration (0, 10, and 20 g/L, respectively). While the samples with the thickness of 120 μm at the same temperature difference exhibited a relatively lower vapor flux (109.4 ± 8, 101.7 ± 6.5 and 96.6 ± 7 kg/m^2·h) from the identical feed conditions, which indicated that the thickness of the membrane became the dominant factor here in spite of the relatively loosely packed network for thicker PS-25 membrane.[1,2,12,41]

For both samples with different thickness, the conductivity of the permeate side remained at a stable low value (~2.4 μs/cm) during the testing periods in the case of the feed solution with 10 and 20 g/L NaCl salt concentration at temperature difference of 55 °C. This obtained high salt rejection and remarkable permeate vapor flux was attributed to the unique hierarchical structure of PS-25 superhydrophobic micro/nano-

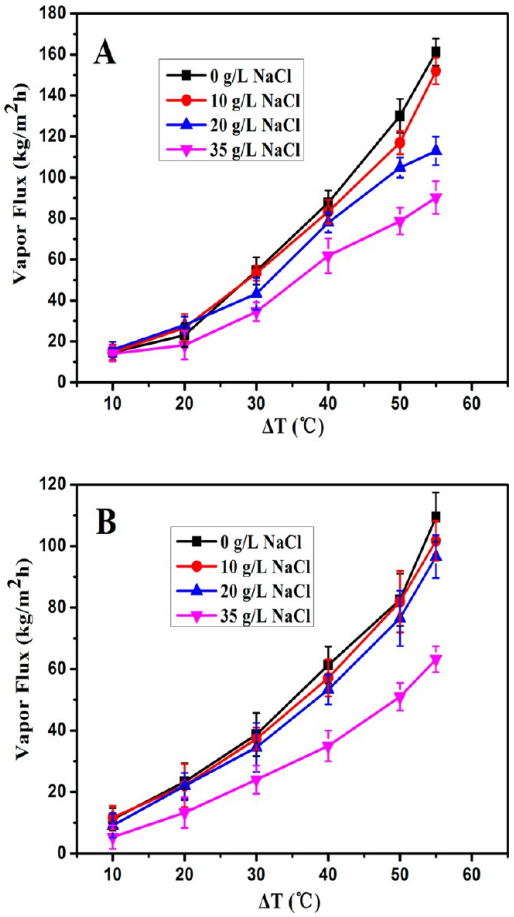

Figure 6. Direct contact MD specific permeate vapor fluxes as a function of temperature difference for the prepared PS-25 nanofibrous membranes with the thickness of 60 (A) and 120 μm (B) at different NaCl salt concentrations.

fibers, as stated previously. Nevertheless, although the PS-25 nanofibrous membrane with the thickness of 60 μm presented a high vapor flux of 90.2 ± 8 kg/m^2·h, the permeate conductivity increased gradually to about 7.8 μs/cm after 2 h (as shown in Figure 7A), indicating that the membrane pores suffered

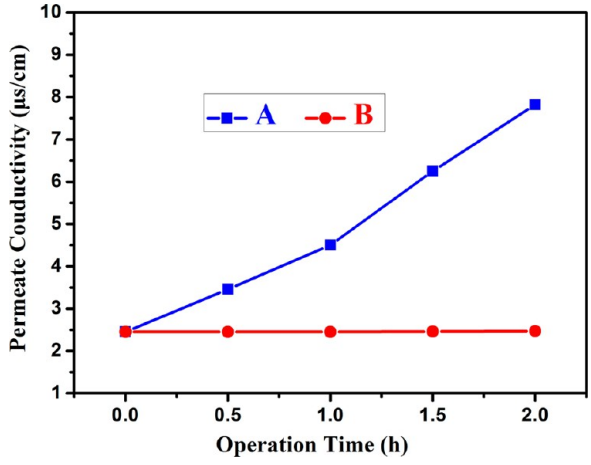

Figure 7. Conductivity changes of the permeate side for PS-25 nanofibrous membranes with the thickness of 60 (A) and 120 μm (B) during testing period of 2 h (ΔT = 55 °C, 35 g/L NaCl salt feed solution).

dx.doi.org/10.1021/am4048128 | ACS Appl. Mater. Interfaces 2014, 6, 2423−2430

wetting due to the concentration polarization effect, when referred to the feed of 35 g/L NaCl salt concentration. While the thicker sample (a thickness of 120 μm) still maintained a stable low permeate conductivity (~2.5 μs/cm) (as shown in Figure 7B) with a vapor flux of 63.2 ± 4.2 kg/m^2·h, which was attributed to its higher LEPw and thickness.

On the basis of the above results, both PS-25 samples with different thickness were performed for different salt solution evaluation. Figure 8 showed the vapor flux and permeate conductivity of the two PS-25 nanofibrous membranes and 0.2 commercial PVDF membrane (mean pore size 0.2 μm) over a period of around 10 h operation. It could be seen that the sample with a thickness of 60 μm maintained a high and stable permeate vapor flux of about 104.8 ± 4.9 kg/m^2·h and a stable low permeate conductivity (~2.4 μs/cm) by employing a 20 g/L NaCl solution as the feed, while the PS-25 sample with a thickness of 120 μm presented a sustainable vapor flux of about 51 ± 4.5 kg/m^2·h and low permeate conductivity (~2.5 μs/cm) from the 35 g/L NaCl salt feed solution with the condition of the temperature difference fixed at 50 °C. The representative FE-SEM images of electrospun PS-25 membranes after MD testing period of 10 h (as shown in Supporting Information Figure S1) confirmed the long-term stability of the fine PS-25 micro/nanoscale hierarchical structures. Consequently, as compared to the desalination efficiency of the 0.2 commercial PVDF membrane (as shown in Figure 8) and PVDF nanofibrous membranes reported so far by Feng et al. (11–12 kg/m^2·h, 35 g/L NaCl salt feed solution, ΔT = 60 °C),[42] Lalia et al. (20–22 kg/m^2·h, 10 g/L NaCl salt feed, ΔT = 40 °C),[38] and Essalhi et al. (54.72 kg/m^2·h, 30 g/L NaCl salt feed, ΔT = 60 °C),[12] the above obtained stable MD performance (permeability and selectivity) suggested PS-25 nanofibrous membranes we demonstrated here could be used as a potential alternative for commercial MD membranes.

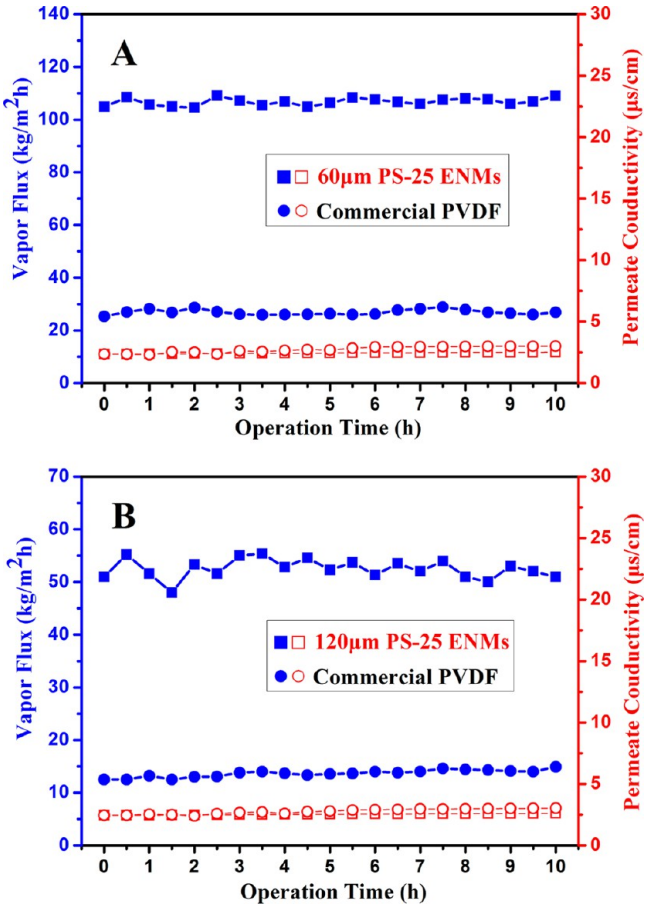

Figure 8. Continuous direct contact MD test of the prepared PS-25 nanofibrous membranes and 0.2 commercial PVDF membrane (mean pore size 0.2 μm): (A) 60 μm, 20 g/L NaCl salt feed solution, (B) 120 μm, 35 g/L NaCl solution as the feed, ΔT = 50 °C, flow rate at feed and permeate side = 0.6 L/min.

CONCLUSION

In summary, we have described the fabrication of a new type of PS superhydrophobic nanofibrous membranes resulting from its dual-biomimetic structure with fine hierarchical roughness. The excellent structural attributes of PS-25 nanofibrous membranes with reasonably high porosity, appropriate MFP and narrow pore size distribution, relatively considerable LEPw value, and fabulous gas permeability were achieved through a series of experiments, fulfilling the requirements of MD application. The direct contact MD evaluation results indicated that these superhydrophobic PS-25 nanofibrous membranes showed superior membrane distillation performance in NaCl solution system, which demonstrated the feasibility of designing and manufacturing novel PS-25 nanofibrous membranes for membrane distillation applications.

ASSOCIATED CONTENT

Supporting Information

The representative FE-SEM images of electrospun PS-25 membranes after MD testing period of 10 h with the condition of the temperature difference fixed at 50 °C confirmed the long-term stability of the fine PS-25 micro/nanoscale hierarchical structures. This information is available free of charge via the Internet at http://pubs.acs.org/.

AUTHOR INFORMATION

Corresponding Authors

*Tel.: +86-21-67792860. Fax: +86-21-67792855. E-mail: wangxf@dhu.edu.cn.

*E-mail: zmf@dhu.edu.cn.

Notes

The authors declare no competing financial interest.

ACKNOWLEDGMENTS

This work was supported by National Science Foundation of China (51273042 and 21174028), Program for New Century Excellent Talents in University, Innovation Program of Shanghai Municipal Education Commission, and Program of Changjiang Scholars and Innovative Research Team in University (IRT1221). We also thank Belgium Porometer company (Guangzhou office, P. R. China) for supporting the characterization by using capillary flow porometer (Porolux 500).

REFERENCES

(1) Alkhudhiri, A.; Darwish, N.; Hilal, N. Membrane Distillation: A Comprehensive Review. *Desalination* **2012**, *287*, 2–18.

(2) Khayet, M. Membranes and Theoretical Modeling of Membrane Distillation: A Review. *Adv. Colloid Interface Sci.* **2011**, *164*, 56–88.

(3) Lawson, K. W.; Lloyd, D. R. Membrane Distillation. *J. Membr. Sci.* **1997**, *124*, 1–25.

(4) Banat, F. A.; Simandl, J. Removal of Benzene Traces from Contaminated Water by Vacuum Membrane Distillation. *Chem. Eng. Sci.* **1996**, *51*, 1257−1265.
(5) Banat, F. A.; Simandl, J. Desalination by Membrane Distillation: A Parametric Study. *Sep. Sci. Technol.* **1998**, *33*, 201−226.
(6) Khayet, M.; Godino, P.; Mengual, J. I. Theory and Experiments on Sweeping Gas Membrane Distillation. *J. Membr. Sci.* **2000**, *165*, 261−272.
(7) Zolotarev, P.; Ugrozov, V.; Volkina, I.; Nikulin, V. Treatment of Waste Water for Removing Heavy Metals by Membrane Distillation. *J. Hazard. Mater.* **1994**, *37*, 77−82.
(8) Ma, Z.; Hong, Y.; Ma, L.; Su, M. Superhydrophobic Membranes with Ordered Arrays of Nanospiked Microchannels for Water Desalination. *Langmuir* **2009**, *25*, 5446−5450.
(9) Phattaranawik, J.; Jiraratananon, R.; Fane, A. Effect of Pore Size Distribution and Air Flux on Mass Transport in Direct Contact Membrane Distillation. *J. Membr. Sci.* **2003**, *215*, 75−85.
(10) Schofield, R.; Fane, A.; Fell, C.; Macoun, R. Factors Affecting Flux in Membrane Distillation. *Desalination* **1990**, *77*, 279−294.
(11) Dzenis, Y. Spinning Continuous Fibers for Nanotechnology. *Science* **2004**, *304*, 1917−1919.
(12) Essalhi, M.; Khayet, M. Self-Sustained Webs of Polyvinylidene Fluoride Electrospun Nanofibers at Different Electrospinning Times: 1. Desalination by Direct Contact Membrane Distillation. *J. Membr. Sci.* **2013**, *433*, 167−179.
(13) Wang, X.; Ding, B.; Yu, J.; Wang, M. Engineering Biomimetic Superhydrophobic Surfaces of Electrospun Nanomaterials. *Nano Today* **2011**, *6*, 510−530.
(14) Gethard, K.; Sae-Khow, O.; Mitra, S. Water Desalination Using Carbon-Nanotube-Enhanced Membrane Distillation. *ACS Appl. Mater. Interfaces* **2011**, *3*, 110−114.
(15) Maab, H.; Francis, L.; Al-Saadi, A.; Aubry, C.; Ghaffour, N.; Amy, G.; Nunes, S. P. Synthesis and Fabrication of Nanostructured Hydrophobic Polyazole Membranes for Low-Energy Water Recovery. *J. Membr. Sci.* **2012**, *423-424*, 11−19.
(16) Prince, J. A.; Singh, G.; Rana, D.; Matsuura, T.; Anbharasi, V.; Shanmugasundaram, T. S. Preparation and Characterization of Highly Hydrophobic Poly(vinylidene fluoride)−Clay Nanocomposite Nanofiber Membranes (PVDF-Clay NNMs) for Desalination Using Direct Contact Membrane Distillation. *J. Membr. Sci.* **2012**, *397-398*, 80−86.
(17) Yoon, H.; Park, J. H.; Kim, G. H. A Superhydrophobic Surface Fabricated by An Electrostatic Process. *Macromol. Rapid Commun.* **2010**, *31*, 1435−1439.
(18) Lu, X.; Zhou, J.; Zhao, Y.; Qiu, Y.; Li, J. Room Temperature Ionic Liquid Based Polystyrene Nanofibers with Superhydrophobicity and Conductivity Produced by Electrospinning. *Chem. Mater.* **2008**, *20*, 3420−3424.
(19) Zhu, Y.; Zhang, J.; Zheng, Y.; Huang, Z.; Feng, L.; Jiang, L. Stable, Superhydrophobic, and Conductive Polyaniline/Polystyrene Films for Corrosive Environments. *Adv. Funct. Mater.* **2006**, *16*, 568−574.
(20) Li, X.; Ding, B.; Lin, J.; Yu, J.; Sun, G. Enhanced Mechanical Properties of Superhydrophobic Microfibrous Polystyrene Mats via Polyamide 6 Nanofibers. *J. Phys. Chem. C* **2009**, *113*, 20452−20457.
(21) Miyauchi, Y.; Ding, B.; Shiratori, S. Fabrication of A Silver-Ragwort-Leaf-like Super-Hydrophobic Micro/Nanoporous Fibrous Mat Surface by Electrospinning. *Nanotechnology* **2006**, *17*, 5151−5156.
(22) Lin, J.; Cai, Y.; Wang, X.; Ding, B.; Yu, J.; Wang, M. Fabrication of Biomimetic Superhydrophobic Surfaces Inspired by Lotus Leaf and Silver Ragwort Leaf. *Nanoscale* **2011**, *3*, 1258−1262.
(23) Casper, C. L.; Stephens, J. S.; Tassi, N. G.; Chase, D. B.; Rabolt, J. F. Controlling Surface Morphology of Electrospun Polystyrene Fibers: Effect of Humidity and Molecular Weight in the Electrospinning Process. *Macromolecules* **2004**, *37*, 573−578.
(24) Megelski, S.; Stephens, J. S.; Chase, D. B.; Rabolt, J. F. Micro- and Nanostructured Surface Morphology on Electrospun Polymer Fibers. *Macromolecules* **2002**, *35*, 8456−8466.
(25) Uyar, T.; Besenbacher, F. Electrospinning of Uniform Polystyrene Fibers: The Effect of Solvent Conductivity. *Polymer* **2008**, *49*, 5336−5343.
(26) Wang, C.; Hsu, C.-H.; Lin, J.-H. Scaling Laws in Electrospinning of Polystyrene Solutions. *Macromolecules* **2006**, *39*, 7662−7672.
(27) Jarusuwannapoom, T.; Hongrojjanawiwat, W.; Jitjaicham, S.; Wannatong, L.; Nithitanakul, M.; Pattamaprom, C.; Koombhongse, P.; Rangkupan, R.; Supaphol, P. Effect of Solvents on Electro-Spinnability of Polystyrene Solutions and Morphological Appearance of Resulting Electrospun Polystyrene Fibers. *Eur. Polym. J.* **2005**, *41*, 409−421.
(28) Jiang, L.; Zhao, Y.; Zhai, J. A Lotus-Leaf-like Superhydrophobic Surface: A Porous Microsphere/Nanofiber Composite Film Prepared by Electrohydrodynamics. *Angew. Chem., Int. Ed.* **2004**, *43*, 4338−4341.
(29) Smolders, K.; Franken, A. C. M. Terminology for Membrane Distillation. *Desalination* **1989**, *72*, 249−262.
(30) Jena, A.; Gupta, K. Characterization of Pore Structure of Filtration Media. *Fluid/Part. Sep. J.* **2002**, *14*, 227−241.
(31) Dullien, F. A. *Porous Media: Fluid Transport and Pore Structure*, 2nd ed; Academic Press: London, 1991.
(32) Martinez, L.; Florido-Diaz, F. Theoretical and Experimental Studies on Desalination Using Membrane Distillation. *Desalination* **2001**, *139*, 373−379.
(33) Martinez-Diez, L.; Florido-Diaz, F.; Vázquez-González, M. Study of Evaporation Efficiency in Membrane Distillation. *Desalination* **1999**, *126*, 193−198.
(34) Shin, Y. M.; Hohman, M. M.; Brenner, M. P.; Rutledge, G. C. Electrospinning: A Whipping Fluid Jet Generates Submicron Polymer Fibers. *Appl. Phys. Lett.* **2001**, *78*, 1149−1151.
(35) Kang, M.; Jung, R.; Kim, H.-S.; Jin, H.-J. Preparation of Superhydrophobic Polystyrene Membranes by Electrospinning. *Colloids Surf., A* **2008**, *313-314*, 411−414.
(36) Kim, K.; Kang, M.; Chin, I.-J.; Jin, H.-J. Unique Surface Morphology of Electrospun Polystyrene Fibers from A N, N-Dimethylformamide Solution. *Macromol. Res.* **2005**, *13*, 533−537.
(37) Wang, L.; Pai, C.-L.; Boyce, M. C.; Rutledge, G. C. Wrinkled Surface Topographies of Electrospun Polymer Fibers. *Appl. Phys. Lett.* **2009**, *94*, 151916−151916-3.
(38) Lalia, B. S.; Guillen-Burrieza, E.; Arafat, H. A.; Hashaikeh, R. Fabrication and Characterization of Polyvinylidenefluoride-co-Hexafluoropropylene (PVDF-HFP) Electrospun Membranes for Direct Contact Membrane Distillation. *J. Membr. Sci.* **2013**, *428*, 104−115.
(39) El-Bourawi, M. S.; Ding, Z.; Ma, R.; Khayet, M. A Framework for Better Understanding Membrane Distillation Separation Process. *J. Membr. Sci.* **2006**, *285*, 4−29.
(40) Liao, Y.; Wang, R.; Tian, M.; Qiu, C. Q.; Fane, A. G. Fabrication of Polyvinylidene Fluoride (PVDF) Nanofiber Membranes by Electro-Spinning for Direct Contact Membrane Distillation. *J. Membr. Sci* **2013**, *425*, 30−39.
(41) Khayet, M.; Matsuura, T. *Membrane Distillation: Principles and Applications*; Elsevier: The Netherlands, 2011.
(42) Feng, C.; Khulbe, K. C.; Matsuura, I.; Gopal, R.; Kaur, S.; Rarnakrishna, S.; Khayet, A. Production of Drinking Water from Saline Water by Air−Gap Membrane Distillation Using Polyvinylidene Fluoride Nanofiber Membrane. *J. Membr. Sci.* **2008**, *311*, 1−6.